MULTI-OUTPUT SPECKLE REDUCTION FILTER FOR ULTRASOUND MEDICAL IMAGES BASED ON MULTIPLICATIVE MULTIRESOLUTION DECOMPOSITION

M.Outtas[⋆†] *L.Zhang*[†] *O.Deforges* [†] *A.Serir*[⋆] *W.Hamidouche*[†]

[⋆] LTIR USTHB, Algeria
[†] IETR INSA Rennes, France

ABSTRACT

Ultrasonographic examination, either as visual inspection or quantitative analysis, is less effective than other medical imaging systems due to speckle noise. The state-of-the-art speckle reduction methods often offers an effective speckle reduction but generally they suffer from oversmoothig, blurring effect and man-made/artificial appearance. In this paper, a new Multi-Output Filter based on a Multiplicative Multiresolution Decomposition (MOF-MMD) is proposed. This multiscale based method, particularly efficient in the case of multiplicative noise, enhances distinctively three outputs: edges, texture and the global image. The multi-output filter aims at offering an enhanced images according to the features desired by radiologists. The different structures, textures and edges are filtered according to the contour image obtained by morphological operators. Finally, we compare the MOF-MMD method with two state-of-the-art speckle reduction methods in terms of speckle reduction capacity and image quality improvement. The results show that the proposed method offers an effective speckle reduction with an improvement of the image quality without blurry and over-smoothing effect.

Index Terms— Speckle reduction, Ultrasound medical images, MMD.

1. INTRODUCTION

Ultrasound(US) is the most widely used medical imaging systems. It is a powerful tool for diagnostic purposes. For more than six decades, ultrasonography has been used to visualize internal body structures such as heart, kidney, tendons, blood vessels and as a guide in surgical procedures. It is safe and painless for the patient, free of radiation risk, portable and inexpensive compared with other imaging modalities (CT or MRI) [1] [2]. It is increasingly viewed as the stethoscope of the future. Ultrasonographic examination is carried out in two ways: qualitative visual inspection based on the clinician's interpretation and quantitative analysis by extracting measures or biomarkers that aid to the diagnosis. In obstetrics, measurement of the nuchal translucency can assess a number of anomalies such as trisomies or congenital heart disease. Moreover, the measurement of Nuchal fold thickness is a marker for Down syndrome with a false positive rate of 1.4% [3]. In cardiology, strain and strain rate are measures of deformation that are descriptors of both the nature and the function of cardiac tissue. These measures can then be used for the assessment of myocardial viability [4]. The Carotid intima-media thickness (CIMT) The intima-media thickness (IMT) is used as a validated measure for the assessment of atherosclerosis In Gastroenterology, liver parenchymal texture is a subjective characteristic for the detection of cirrhosis [5]. Nevertheless, one principal drawback of the US image is that it shows granular structure called speckle. Speckle is an undesirable property of the image as it masks small differences in gray level [6] [7]. This specific artifact: US artifacts, corrupts the image in a multiplicative manner. It appears due to interference phenomena between the incident and reflected signals, and is inherent to US [8]. Speckle appears as a light and dark mottled grainy pattern. It reduces both image contrast and the distinction of subtle gradations and boundaries in tissue structure [1]. The speckle can potentially lead to misinterpretation of the image. It also impedes post-processing techniques such as image segmentation, registration, data classification and texture analysis.

A large number of researches were proposed in order to reduce speckle and/or improve the quality of US images. Post-processing speckle reduction techniques are widely used. Indeed, as multiplicative speckle noise corrupts the synthetic aperture radar (SAR) images in the same manner as it does on US images, many speckle reducing filters originated from the SAR community were used for US images such as Median filter [9], Wiener filter, Lee filter [10] [11] or Frost filter [12]. On the other hand, several approaches have been proposed to reduce more specifically the speckle on US medical images. These approaches can be classified into the following categories [13]: anisotropic diffusion filter [14] [15], multi-scale filter [16], non-local means filter [17], and hybrid filter [18].

Speckle reduction techniques present some limitations such as texture over-smoothing, loss of subtle details during the filtering process or moreover edge blurring. Some filtering methods also give artificial appearance to the enhanced images [13]. However, all the speckle reduction works propose a unique viewing possibility, while the interpretation of an US is based on multiple evaluation tasks: general aspect, echo patten, outer contour/border and size. To encounter this problem, we propose in this paper a Multi-Output Filter based on Multiplicative Multiresolution Decomposition (MOF-MMD), which performs speckle reduction in order to enhance the relevant structures and textures (edges, texture and the global image) according to different diagnosis needs.

The paper is structured as follows: In section 2 a brief description of the above mentioned MMD is addressed. The proposed method and implementation are detailed in Section 3. In Section 4 experiments and results are carried out by comparing the method with the previously cited speckle filters. Conclusions are summarized in Section 5.

2. MULTIPLICATIVE MULTIRESOLUTION DECOMPOSITION (MMD)

The nonlinear multiplicative decomposition is a multi-scale analysis/synthesis representation of 2D signals [19]. This nonlinear decomposition is suitable for a multiplicative noise reduction and has been used to reduce multiplicative noise in Synthetic Aperture Radar [19] and medical US images [20]. It uses filter banks

with critical sub-sampling and perfect reconstruction. In [19] the authors consider a description of the analysis and the synthesis inputs-outputs systems with equal symbol rates at both the input and the output. The wanted structure is obtained by performing a polyphase decomposition of the 2D signal (the image) [21]. Thus the image is decomposed into an approximate output subband y_1 and three nonlinear outputs details y_{2H}, y_{2V}, y_{2D} vary within the interval $[0, 1]$.

The MMD's coefficients are normally distributed around β which is a positive scalar. High contrasted details correspond to values far from β, whereas values close to β correspond to smooth regions. The value of β is set to 0.5. In the rest of the paper, we will refer to all the details y_{2H}, y_{2V}, y_{2D} by D_C where C stands for $'H'$ horizontal, $'V'$ vertical and $'D'$ Diagonal details. The multiresolution decomposition is than based on sub-band decomposition. The sub-band $y_1^{(j)}$ at a resolution $j \in [1, J]$ is split into its polyphase components and then filtered. At the highest resolution J, the original image is represented by the set R defined by $R = \left(y_1{}^{(j)}, \left(y_{2h}{}^{(j)}, y_{2v}{}^{(j)}, y_{2d}{}^{(j)}\right)\right)_{2 \leq j \leq J}$. The original image is perfectly reconstructed by using multiresolution synthesis scheme detailed in [19].

3. METHODOLOGY

The proposed MOF-MMD is schematically represented in Fig. 1. It is consists of five steps: 1) a preliminary step of features-like segmentation achieved using morphological operators; 2) the noise level is calculated from local window; 3) a multi-scale decomposition is performed using MMD; 4) three thresholding are applied according to the features; 5) enhanced images reconstruction using MMD. Finally, outputs are validated according to quality measure criterion. The details of each step is given bellow.

a. Features-like segmentation by morphological operator

In this paper we aim to reduce the speckle in US images while preserving the edge and details. Thus, it is important to bring out the different features or structures of the image. We use morphological operators to segment features-like structure. Indeed, morphological operators perform better and faster than the standard approaches in pre-processing and segmentation using object shape [22]. To perform morphological transformation, a shape parameters called a structuring element (SE), characterized by its shape and size, is used. As medical images generally contain more round shapes than straight lines and angles, the disk-shaped structuring element is more appropriate choice. An algorithm for an efficient computation of morphological operations for gray images with a circular structuring element is proposed in [23].

Let I be the original US image and C the circular structuring element with a radius of eight pixels. The features-like segmentation is obtain as follows:

$$I_{(o)} = I \circ C \tag{1}$$

$$I_{(oc)} = I_{(o)} \bullet C \tag{2}$$

$$I_{(e)} = I_{(oc)} \ominus C \tag{3}$$

$$I_{(d)} = I_{(oc)} \oplus C \tag{4}$$

$$S = I_{(d)} - I_{(e)} \tag{5}$$

where $\oplus$, $\ominus$, $\circ$ and $\bullet$ denote dilatation, erosion, opening and closing operators, respectively. S represents the contour image obtained by morphological treatment and showed in Fig. 2(b).

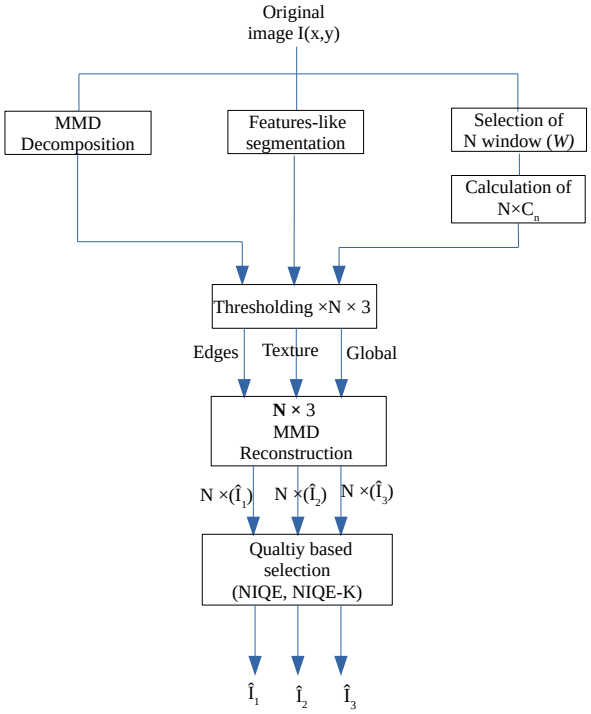

Fig. 1. MOF-MMD Diagram

b. Selection of W and calculation of C_n

The proposed multi-scale filter performs a thresholding of each coefficient D_C at all scales J. The threshold T is computed from the noise level C_n, which is calculated from the variance and the mean of a local window W of constant intensity selected by the user $C_n^2 = \frac{var_W}{\mu_W}$.

In order to ensure selecting of the best C_n and consequently the best threshold T, a number N of window W are selected in this work. The Fig. 3 shows 3 selected window ($N = 3$), for calculation of C_n and T.

c. Thresholding: Multi-Output filter

As indicated in Section 2, in smooth regions the values of the MMD'S coefficients components are close to β. This property

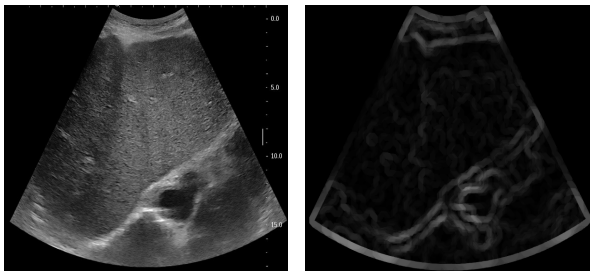

(a) Original image (b) Contour image

Fig. 2. Features-like segmentation

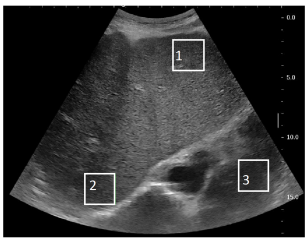

Fig. 3. Local windows selected for calculation of C_n and T

helps to enhance the image while preserving structural details and avoiding blurring effect. In order to permit multiple enhancement possibilities of the original US image, the thresholding is done according to pixel intensity of the images obtained from features-like segmentation.

c.1. Filter first output - Sharp edge enhancement

This first output of the filter is an image with enhanced edges. It is pertinent for measures conducted in US images such as lesion size, distance and so on. For each pixel of the contour image a thresholding is applied as following

$$\hat{D}_C^{(j)} = \begin{cases} \beta \quad if \qquad \beta - \beta_t \leq D_C^{(j)} \leq \beta + \beta_t \\ D_C^{(j)} \times \nu - (\gamma \times \alpha \times S) \quad if \quad D_C^{(j)} + \tau \leq \beta \\ D_C^{(j)} \times \nu + (\gamma \times \alpha \times S) \quad if \quad D_C^{(j)} - \tau \geq \beta \\ \beta \quad otherwise \end{cases} \tag{6}$$

where $D_C^{(j)}$ and $\hat{D}_C^{(j)}$ represent the MMD's coeficient at scale j of the original noisy I image and its thresholded version respectively. β_t is a threshold that aim to reduce speckle of the coefficients components in the smoothest pixels. $\tau = (T \times \nu \times \alpha \times S)$, with $T = C_n \times j/J$ is the threshold calculated from noise level at each scale j with J represent the number of scales. α is set to 0.25 to avoid the displacement of edge pixels in the filtered images. ν and γ are given by $\nu = \frac{1}{\sqrt{1+{C_n}^2}}$ and $\gamma = 1 - \frac{1}{\sqrt{1+{C_n}^2}}$. Notice that the thresholding is proportional to contour images *i.e.* more important is the edges more it is enhanced.

c.2. Filter second output - Texture enhancement

This second output of the filter is an image with enhanced texture. It is pertinent for enhance texture by reducing speckle while preserve the texture pattern. Let $\bar{S}$ denotes the image of pixels that do not belong to the contour S. The second output results from the following thresholding

$$\hat{D}_C^{(j)} = \begin{cases} \beta \quad if \qquad \beta - \beta_t \leq D_C^{(j)} \leq \beta + \beta_t \\ D_C^{(j)} \times \nu - \left(\gamma \times \bar{S}\right) \quad if \quad D_C^{(j)} + \xi \leq \beta \\ D_C^{(j)} \times \nu + \left(\gamma \times \bar{S}\right) \quad if \quad D_C^{(j)} - \xi \geq \beta \\ \beta \quad otherwise \end{cases} \tag{7}$$

with $\xi = \left(T \times \nu \times \bar{S}\right)$,

c.3. Filter third output - Global image enhancement

The third output of the filter is a global enhancement of the image. Based on the complement of the image contour Co_S . The MMD's coefficients are thresholded according to the scheme of the Co_S image, as follow:

$$\hat{D}_C^{(j)} = \begin{cases} \beta \quad if \qquad \beta - \beta_t \leq D_C^{(j)} \leq \beta + \beta_t \\ D_C^{(j)} \times \nu - (\gamma \times Co_S) \quad if \quad D_C^{(j)} - (\gamma \times Co_S) \leq \beta \\ D_C^{(j)} \times \nu + (\gamma \times Co_S) \quad if \quad D_C^{(j)} + (\gamma \times Co_S) \geq \beta \\ \beta \quad otherwise \end{cases} \tag{8}$$

d. MMD reconstruction and quality based selection

The three obtained $\hat{D}_C^{(J)}$ are reconstructed by MMD synthesis into enhanced image $\hat{I}_1, \hat{I}_2, \hat{I}_3$.

In the case of $N \times C_n$, we will obtain $N \times \left\{\hat{I}_1, \hat{I}_2, \hat{I}_3\right\}$. The three final enhanced images $\hat{I}_1, \hat{I}_2, \hat{I}_3$ are chosen according to quality measure criterion: NIQE and NIQE-K. These metrics are defined later in subsection 4-b. For the US image represented in Fig. 3, the C_n of 2^{nd} window is selected as best value for enhancing the represented US image.

4. EXPERIMENTS AND RESULTS

In this section, the proposed filter is compared with two recent and efficient speckle reduction filters: Optimized Bayesian NL-Means with block selection (OBNLM) [17] and Anisotropic Diffusion filter with Memory based on Speckle Statistics(ADMSS) [15]. This comparison is carried out in terms of the speckle reduction capacity and the improvement of the image quality.

a. Experimental images

In order to evaluate the despeckeling filter, we used clinical US images of *in vivo* abdominal liver. We obtained 21 US images of symptomatic and asymptomatic liver with different resolution, from a retrospective database of the University Hospital of Angers. The US system used to capture these images is the SuperSonic Aixplorer and the Siemens Acuson S2000. The images were registered and processed offline.

b. Evaluation metrics

In order to quantify the speckle reduction achieved by different filters, speckle's signal-to-noise ratio (SSNR) is measured [18]. It is measured in a fully formed region and expressed by

$$SSNR = \frac{\mu}{\sigma} \tag{9}$$

where μ is the mean intensity value and σ is the standard deviation in the region of fully formed speckle. A higher value of the SSNR indicates less speckle.

Three image quality evaluation metrics were also chosen to assess the quality of the filtered images. As there is no genuine reference image for medical images, it is interesting to use blind metrics. In this paper, we use two state-of-the-art no-reference metrics (NIQE [24] and BIQES [25]) and our previously proposed blind metric NIQE-K [26], defined in the following :

$$NIQE = \sqrt{\left((\nu_1 - \nu_2)^T \left(\frac{\sum_1 + \sum_2}{2}\right)(\nu_1 - \nu_2)\right)} \tag{10}$$

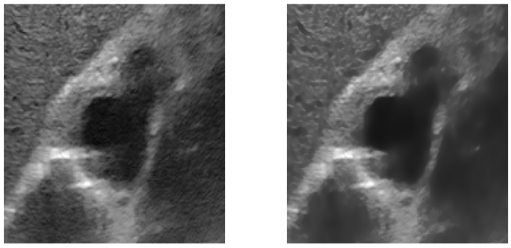

(a) Original noisy image

(b) ADMSS

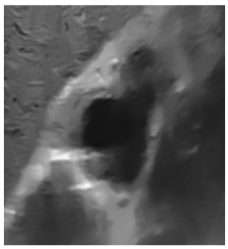

(c) OBNLM

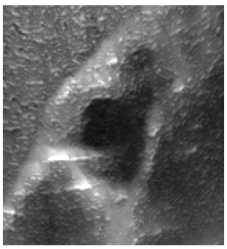

(d) MOF-MMD 1^{st}: edges

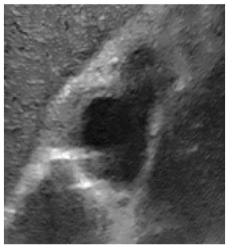

(e) MOF-MMD 2^{nd}: texture

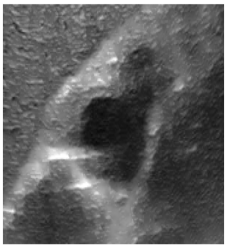

(f) MOF-MMD 3^{rd}: global

Fig. 4. Comparison of speckle reductions of liver US image

where ν_1, ν_2 and $\sum_1, \sum_2$ are the mean vectors and covariance matrices of the reference image's multivariate Gaussian (MVG) model and the distorted image's MVG model, respectively.

$$BIQES = \frac{k}{\sigma}\overline{Q_L} + \sigma\overline{Q_H} \tag{11}$$

where k and σ are the *kurtosis* and the *standard deviation* of log amplitude of the image's Fourier spectra, respectively. $\bar{\cdot}$ denotes the mean operation of Q_L and Q_H the calculated low pass error and high pass error.

$$NIQE - K = NIQE \times \frac{k}{\sigma} \tag{12}$$

A lower value of the metrics indicates a better quality of the image.

c. Results and discussion

We can see that MOF-MMD's output1 shows an enhancement of the hepatic vessel (the hyper-echogenic line. cf. Fig. 4(d)); MOF-MMD's output 2 enhanced the texture while reducing the speckle (cf. Fig. 4(e)); the MOF-MMD's output 3 offers an overall enhancement of the noisy image(cf. Fig. 4(f)). Compared to our method, the OBNLM reveals an over-smoothing of the feature: the texture/grainy appearance which helps to the diagnose is completely deleted. The ADMSS smooths the speckled image gradually and preserves the edges satisfactorily, but it also removes the structural details since its memory function considers them to be meaningless regions.

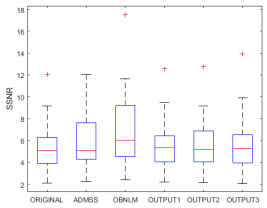

(a) SSNR

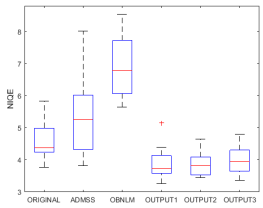

(b) NIQE

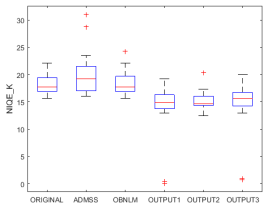

(c) NIQE-K

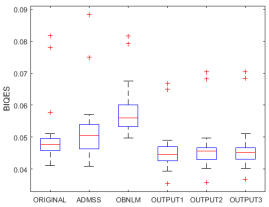

(d) BIQES

Fig. 5. Box plots of SSNR and quality assessment metrics of US images and their filtered versions:ADMSS, OBNLM, Proposed OUTPUT1-3. (A higher SSNR indicates less speckle. The lower values of metrics means higher performances)

For objective comparison, the SSNR and the three evaluation metrics are calculated and depicted with box plot in Fig. 5. Considering the speckle reduction capacity showed by the SSNR in Fig. 5(a), the proposed method as well as the OBNLM and ADMSS reduce the speckle with a bit better performance for the OBNLM filter. In terms of quality improvement, the three metrics indicate that the OBNLM filter offers worst performance due to over-smoothing effect. Regarding the three outputs of the proposed method, the NIQE,NIQE-K and BIQES indicate a significantly higher quality comparing to the OBNLM and the ADMSS. Moreover, the standard deviations of the three output are lower than those of the ADMSS and OBNLM, which indicate a lower dispersion and a higher uniformity of the processed images. The MOF-MMD substantially reduces the speckle while improving the quality of the image. It provides three outputs useful for the diagnosis of general aspect, echo patten and outer border.

5. CONCLUSION

In this paper, we propose a new speckle reduction multi-scale approach based on multiplicative multiresoution decomposition (MOF-MMD). It enhances different features and structures of the images previously extracted by mathematical morphology operators. Experimental results demonstrate that the proposed method effectively reduces the speckle and improves the quality of the US images by enhancing the boundaries of lesions and reducing the speckle in the echo texture of organs while preserving the pattern without neither over-smoothing nor artificial appearance. While this multi-output method has a general good performance, it can also respond to different special needs of radiologists with different outputs which has a potential to ameliorate their diagnostic task. To further valid our proposed method, we will evaluate its performances by subjective tests.

6. REFERENCES

[1] Thomas L Szabo, *Diagnostic ultrasound imaging: inside out*, Academic Press, 2004.

[2] J. A. Jensen, "Medical ultrasound imaging," *Progress in Biophysics and Molecular Biology*, vol. 93, no. 13, pp. 153 – 165, 2007, Effects of ultrasound and infrasound relevant to human health.

[3] A. Locatelli, M. G. Piccoli, P. Vergani, E. Mariani, A. Ghidini, S Mariani, and John C. Pezzullo, "Critical appraisal of the use of nuchal fold thickness measurements for the prediction of down syndrome," *American Journal of Obstetrics and Gynecology*, vol. 182, no. 1, pp. 192 – 197, 2000.

[4] Thomas H. Marwick, "Measurement of strain and strain rate by echocardiographyready for prime time?," *Journal of the American College of Cardiology*, vol. 47, no. 7, pp. 1313–1327, 2006.

[5] J. F. Gerstenmaier and R. N. Gibson, "Ultrasound in chronic liver disease," *Insights into imaging*, vol. 5, no. 4, pp. 441–455, 2014.

[6] Christoph B Burckhardt, "Speckle in ultrasound b-mode scans," *Sonics and Ultrasonics, IEEE Transactions on*, vol. 25, no. 1, pp. 1–6, 1978.

[7] R. F. Wagner, S. W. Smith, J. M. Sandrik, and H. Lopez, "Statistics of Speckle in Ultrasound B-Scans," *Sonics and Ultrasonics, IEEE Transactions on*, vol. 30, no. 3, pp. 156–163, 1983.

[8] A. C. Frery, H. J. Müller, C. C. F. Yanasse, and S. J. S. Sant'Anna, "A model for extremely heterogeneous clutter," *IEEE T. Geoscience and Remote Sensing*, vol. 35, no. 3, pp. 648–659, 1997.

[9] E. Ritenour, T. Nelson, and U. Raff, "Applications of the median filter to digital radiographic images," in *Acoustics, Speech, and Signal Processing, IEEE International Conference on ICASSP '84.*, Mar 1984, vol. 9, pp. 251–254.

[10] J. S. Lee, "Digital image enhancement and noise filtering by use of local statistics," *IEEE Transactions on Pattern Analysis and Machine Intelligence*, vol. PAMI-2, no. 2, pp. 165–168, March 1980.

[11] J. S. Lee, "Speckle analysis and smoothing of synthetic aperture radar images," *Computer graphics and image processing*, vol. 17, no. 1, pp. 24–32, 1981.

[12] V. S. Frost, J. A. Stiles, K. S. Shanmugan, and J. Holtzman, "A model for radar images and its application to adaptive digital filtering of multiplicative noise," *Pattern Analysis and Machine Intelligence, IEEE Transactions on*, , no. 2, pp. 157–166, 1982.

[13] J. Zhang, C. Wang, and Y. Cheng, "Comparison of despeckle filters for breast ultrasound images," *Circuits, Systems, and Signal Processing*, vol. 34, no. 1, pp. 185–208, 2015.

[14] Yongjian Yu and Scott T Acton, "Speckle reducing anisotropic diffusion," *IEEE Transactions on image processing*, vol. 11, no. 11, pp. 1260–1270, 2002.

[15] Gabriel Ramos-Llordén, Gonzalo Vegas-Sánchez-Ferrero, Marcos Martin-Fernandez, Carlos Alberola-López, and Santiago Aja-Fernández, "Anisotropic diffusion filter with memory based on speckle statistics for ultrasound images," *IEEE Transactions on Image Processing*, vol. 24, no. 1, pp. 345–358, 2015.

[16] A. Pizurica, W. Philips, I. Lemahieu, and M. Acheroy, "A versatile wavelet domain noise filtration technique for medical imaging," *IEEE Trans. Med. Imaging*, vol. 22, no. 3, pp. 323–331, 2003.

[17] P. Coupé, P. Hellier, C. Kervrann, and C Barillot, "Nonlocal means-based speckle filtering for ultrasound images," *IEEE Transactions on Image Processing*, vol. 18, pp. 2221–2229, 2009.

[18] J. Kang, J. Young Lee, and Y. Yoo, "A new feature-enhanced speckle reduction method based on multiscale analysis for ultrasound b-mode imaging," *IEEE Transactions on Biomedical Engineering*, vol. 63, no. 6, pp. 1178–1191, 2016.

[19] A. Serir and A. Belouchrani, "Multiplicative multiresolution decomposition for 2d signals: application to speckle reduction in sar images," in *Image Processing, 2004. ICIP '04. 2004 International Conference on*, Oct 2004, vol. 1, pp. 657–660 Vol. 1.

[20] M. Outtas, A. Serir, and F. Kerouh, "Speckle noise reduction in ultrasound image based on A Multiplicative Multiresolution Decomposition (MMD)," in *ISIVC 2014*, Marrakech, Morocco, Nov., The eighth edition of International Symposium on signal, Image, Video and Communications (ISIVC).

[21] A. Serir, A. Beghdadi, and F. Kerouh, "No-reference blur image quality measure based on multiplicative multiresolution decomposition," *Journal of Visual Communication and Image Representation*, vol. 24, no. 7, pp. 911 – 925, 2013.

[22] M. Sonka, V. Hlavac, and R. Boyle, *Image Processing, Analysis, and Machine Vision*, Thomson-Engineering, 2007.

[23] O. Déforges, N. Normand, and M. Babel, "Fast recursive grayscale morphology operators: from the algorithm to the pipeline architecture," *Journal of Real-Time Image Processing*, vol. 8, no. 2, pp. 143–152, 2013.

[24] A. Mittal, R. Soundararajan, and A. C. Bovik, "Making a "completely blind" image quality analyzer," *IEEE Signal Process. Lett.*, vol. 20, no. 3, pp. 209–212, 2013.

[25] Ashirbani Saha and Qing Ming Jonathan Wu, "Utilizing image scales towards totally training free blind image quality assessment," *Image Processing, IEEE Transactions on*, vol. 24, no. 6, pp. 1879–1892, 2015.

[26] M. Outtas, L. Zhang, O. Deforges, W. Hamidouche, A. Serir, and C. Cavaro-Menard, "A study on the usability of opinion-unaware no-reference natural image quality metrics in the context of medical images," in *ISIVC 2016*, International Symposium on Signal, Image, Video and Communications.